

# **Multipath fading demonstration using software defined radio**

Naoki Sean Pross

Sara Cinzia Halter

Fall semester 2021



## Abstract

[Redacted text block consisting of 12 horizontal bars]



# Contents

<b>1</b>	<b>Introduction</b>	<b>1</b>
1.1	Background . . . . .	1
1.2	Task description . . . . .	1
1.3	Overview . . . . .	2
<b>2</b>	<b>Theory</b>	<b>3</b>
2.1	Overview . . . . .	3
2.2	Quadrature amplitude modulation ( $M$ -ary QAM) . . . . .	3
2.2.1	Modulation of a digital message . . . . .	3
2.2.2	Orthogonality of carrier signals . . . . .	5
2.2.3	Construction of orthogonal carrier signals . . . . .	7
2.2.4	Spectral properties of a QAM signal . . . . .	7
2.3	Phase shift keying ( $M$ -PSK) . . . . .	7
2.3.1	Quadrature PSK (QPSK) . . . . .	7
2.4	Wireless channel . . . . .	8
2.4.1	Geometric multipath fading model . . . . .	8
2.4.2	Spectrum of a multipath fading channel . . . . .	10
2.4.3	Discrete-time model . . . . .	10
2.4.4	Difficulties caused by discrete time . . . . .	12
2.4.5	Statistical model . . . . .	13
<b>3</b>	<b>Implementation</b>	<b>15</b>
3.1	Overview . . . . .	15
3.2	Sender chain . . . . .	15
3.2.1	Data source . . . . .	15
3.2.2	Modulation . . . . .	15
3.3	Receiver chain . . . . .	15
3.3.1	Envelope detector . . . . .	15
3.3.2	Frame synchronization . . . . .	16
3.4	Channel simulations . . . . .	16
3.5	Hardware . . . . .	17
3.5.1	Empirical BER . . . . .	17
3.5.2	Measurements . . . . .	17

*Contents*

**4 Conclusions**

**21**

# 1 Introduction

## 1.1 Background

It is undeniable that in the last two decades modern wireless devices have become extremely ubiquitous, and are no longer employed under carefully chosen conditions.

Nowadays smart phones and internet of things (IoT) devices and many other wireless devices are carried around by everyone and have to work in environments that are very far from ideal. Furthermore in addition to the already large class of networked appliances, next generation wireless devices in urban environments will include the new category of vehicles [1], where reliability of intra-vehicular communication directly translates into safety. While at the same time in rural regions, developing countries as well as other low-user density areas wireless transmission links using mesh networks have become a practical alternative to wired broadband [9, 12, 2].

The study of problems concerning wireless devices is thus a very relevant topic today. More specifically, a common issue in the previously mentioned use cases is the so called *multipath fading effect*, which degrades the reliability of the transmission link [11, 5]. The presence of fading was actually foreseen [3, 10] and today most modern transmission schemes implement measures to reduce the effects of fading [11, 6].

This work studies the multipath fading effect, and how it affects modern digital transmission systems that use quadrature amplitude modulation (QAM) and phase shift keying (PSK) modulation.

## 1.2 Task description

As described in the document given at the beginning of the semester:

The goal is to develop a SDR-based demonstrator, consisting of one transmitter and one receiver, to illustrate the impact of different fading effects on the signal. To get a brief understanding of the concept of fading channels, the project should be started with a literature research followed by simulation of different scenarios, which then can be reproduced by measurements.

The task description document is found in the appendix.

## 1.3 Overview

1





## 2 Theory

The first two sections will briefly give the mathematics required by the modulation schemes used in the project. The notation used is summarised in Fig. 2.1. For conciseness encoding schemes and (digital) signal processing calculations are left out and discussed later. Thus for this section  $m_e = m$ .

2

3

### 2.1 Quadrature amplitude modulation ( $M$ -ary QAM)

Quadrature amplitude modulation is a family of modern digital modulation methods, that use an analog carrier signal. The simple yet effective idea behind QAM is to encode extra information into an orthogonal carrier signal, thus increasing the number of bits sent per unit of time [5, 7, 11, 6]. A block diagram of the process is shown in Fig. 2.2.

#### 2.1.1 Modulation of a digital message

**Bit splitter** As mentioned earlier, quadrature modulation allows sending more than one bit per unit time. The first step to do it is to use a so called bit splitter, that converts the continuous bitstream  $m(n)$  into pairs of chunks of  $\sqrt{M}$  bits. The two bit vectors of length  $\sqrt{M}$ , denoted by  $\mathbf{m}_i$  and  $\mathbf{m}_q$  in figure 2.2, are called in-phase and quadrature component respectively[6]. The reason will become more clear later.

**Binary to level converter** Both bit vectors  $\mathbf{m}_i, \mathbf{m}_q \in \{0, 1\}^{\sqrt{M}}$  are sent through a binary to level converter. It's purpose is to reinterpret the bit vectors as numbers, usually in gray code, and to convert them into analog waveforms, which we will denote with  $m_i(t)$  and  $m_q(t)$  respectively. Mathematically the binary to level converter can be described as:

$$m_i(t) = \text{Level}(\mathbf{m}_i) \cdot p(t), \quad (2.1)$$

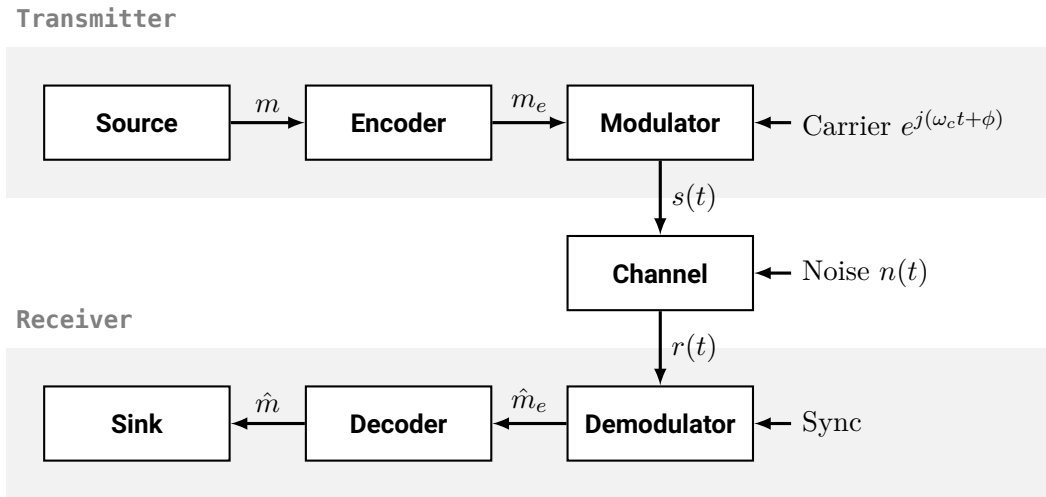


**Figure 2.1** Block diagram for a general wireless communication system with annotated signal names. Frequency domain representations of signals use the uppercase symbol of their respective time domain name.

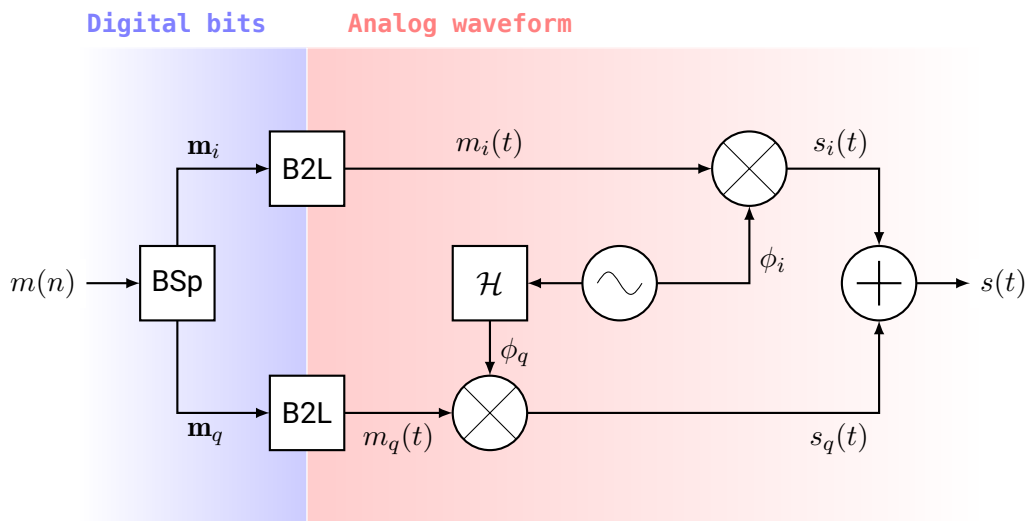


**Figure 2.2** Block diagram of a  $M$ -ary QAM modulator.

## 2.1 Quadrature amplitude modulation ( $M$ -ary QAM)

i.e. a pulse function<sup>1</sup>  $p(t)$  scaled by the interpreted binary value, written here using a “Level” function. So at this point a level of each analog waveform is encodes  $\sqrt{M}$  bits per unit time, and there are two of such waveforms.

**Mixer** Having analog level signals, it is this now possible to mix them with radio frequency carriers. Because there are two waveforms, one might expect that two carrier frequencies are necessary, however this is not the case. The two component  $m_i(t)$  and  $m_q(t)$  are mixed with two different periodic signals  $\phi_i(t)$  and  $\phi_q(t)$  that have the same frequency  $\omega_c = 2\pi/T$ . How this is possible is explained in the next section.

### 2.1.2 Orthogonality of carrier signals

Before explaining how the two carrier signals are generated, we first need to discuss some important mathematical properties  $\phi_i$  and  $\phi_q$  need to have, in order to modulate two messages over the same frequency  $\omega_c$ . The two carriers need to be *orthonormal*<sup>2</sup> to each other, mathematically this is expressed by the conditions

$$\langle \phi_i, \phi_q \rangle = \int_T \phi_i \phi_q^* dt = 0, \text{ and} \quad (2.2a)$$

$$\langle \phi_k, \phi_k \rangle = \int_T \phi_k \phi_k^* dt = 1, \text{ where } k \text{ is either } i \text{ or } q. \quad (2.2b)$$

Provided these rather abstract conditions, let’s define a new signal

$$s = m_i \phi_i + m_q \phi_q. \quad (2.3)$$

Notice that assuming  $m_i$  and  $m_q$  are constant<sup>3</sup> over the carrier’s period  $T$ ,

$$\begin{aligned} \langle s, \phi_i \rangle &= \int_T s \phi_i^* dt = \int m_i \phi_i \phi_i^* + m_q \phi_q \phi_i^* dt \\ &= m_i \underbrace{\int_T \phi_i \phi_i^* dt}_1 + m_q \underbrace{\int_T \phi_q \phi_i^* dt}_0 = m_i, \end{aligned}$$

which effectively means that it is possible to isolate a single component  $m_i(t)$  out of  $s(t)$ . The same of course works with  $\phi_q$  as well resulting in  $\langle s, \phi_q \rangle = m_q$ . Thus (remarkably) it is possible to send two signals on the same frequency, without them interfering with each other. Since each signal can represent one of  $\sqrt{M}$  values, by having two we obtain  $\sqrt{M} \cdot \sqrt{M} = M$  possible combinations.

<sup>1</sup>Typically a root raised cosine to optimize for bandwidth [6].

<sup>2</sup>Actually orthogonality alone would be sufficient, however then the left side of (2.2b) would not equal 1, and an inconvenient factor would be introduced in many later equations [5, 6].

<sup>3</sup>This is an approximation assuming that the signal changes much slower relative to the carrier.

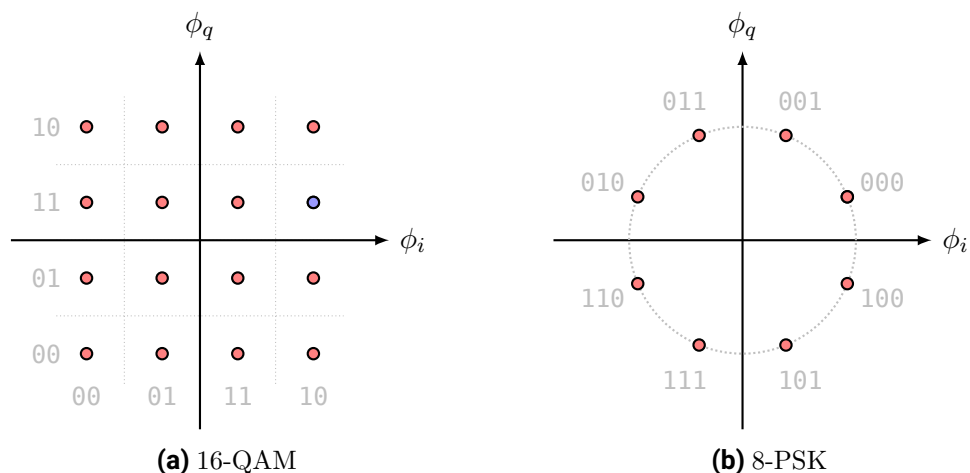


**Figure 2.3** Examples of constellation diagrams. Each dot represents a possible location for the complex amplitude of the passband signal.

A graphical way to see what is happening, is to observe a so called *constellation diagram*. An example is shown in Fig. 2.3(a) for  $M = 16$ . The two carrier signals  $\phi_i$  and  $\phi_q$  can be understood as bases of a coordinate system, in which the two amplitude levels of the two modulated messages, determine a position in the grid.

**Example** A concrete example for  $M = 16$ : if the message is 1110 the bit splitter creates two values  $\mathbf{m}_q = 11$  and  $\mathbf{m}_i = 10$ ; both are converted into analog amplitudes  $m_q = 3$  and  $m_i = 4$ ; that are then mixed with their respective carrier, resulting in  $s(t)$  being the point inside the bottom right sub-quadrant of the top right quadrant (blue dot in Fig. 2.3(a)).

In Fig. 2.3(a) the dots of the constellation have coordinates that begin on the bottom left corner, and are nicely aligned on a grid. Both are not a necessary requirement for QAM, in fact there are many schemes (for example when  $M = 32$ ) that are arranged on a non square shape, and place the dots in different orders. The only constraint that most QAM modulators have in common, with regards to the geometry of the constellation, is that between any two adjacent dots (along the axis, not diagonally) only one bit of the represented value changes (gray code). This is done to improve the bit error rate (BER) of the transmission.

### 2.1.3 Construction of orthogonal carrier signals

Knowing why there is a need for orthogonal carriers, we should now discuss which functions satisfy the property described by (2.2a). If  $\phi_i$  is a real valued signal (which

## 2.2 Phase shift keying ( $M$ -PSK)

is typical) it is possible to find a function the quadrature carrier using the *Hilbert transform* (sometimes called Hilbert filter):

$$\mathcal{H}g(t) = g(t) * \frac{1}{\pi t} = \frac{1}{\pi} \int_{\mathbb{R}} \frac{g(\tau)}{t - \tau} d\tau = \frac{1}{\pi} \int_{\mathbb{R}} \frac{g(t - \tau)}{\tau} d\tau. \quad (2.4)$$

The Hilbert transform is a linear operator that introduces a phase shift of  $\pi/2$  over all frequencies [6, 5], and it is possible to show that given a real valued function  $g(t)$  then  $\langle g, \mathcal{H}g \rangle = 0$  [8, 7]. There are many functions that are Hilbert transform pairs, however in practice the pair  $\phi_i(t) = \cos(\omega_c t)$  and  $\phi_q(t) = \mathcal{H}\phi_i(t) = \sin(\omega_c t)$  is always used.

### Oscillator and phase shifter

4

#### 2.1.4 Spectral properties of a QAM signal

5

## 2.2 Phase shift keying ( $M$ -PSK)

6

### 2.2.1 Quadrature PSK (QPSK)

7

## 2.3 Wireless channel

In the previous section, we discussed how the data is modulated and demodulated at the two ends of the transmission system. This section discusses what happens between

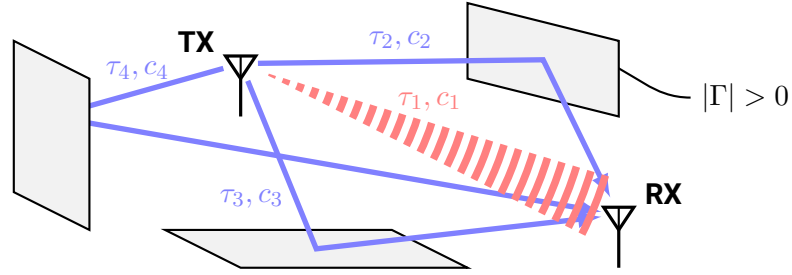


**Figure 2.4** Sketch of channel with multipath fading.

the sender and receiver when the modulated passband signal is transmitted wirelessly.

In theory because wireless transmission happens through electromagnetic radiation, to model a wireless channel one would need to solve Maxwell’s equations for either the electric or magnetic field, however in practice that is not (analytically) possible. Instead what is typically done, is to model the impulse response of the channel using a geometrical or statistical model, parametrized by a set of coefficients that are either simulated or measured experimentally [5].

In our model we are going to include an additive white Gaussian noise (AWGN) and a Rician (or Rayleigh) fading; both are required to model physical effects of the real world. The former in particular is relevant today, as it mathematically describes dense urban environments.

### 2.3.1 Geometric multipath fading model

The simplest way to understand the multipath fading, is to consider it from a geometrical perspective. Fig. 2.4 is a sketch a wireless transmission system affected by multipath fading. The sender’s antenna radiates an electromagnetic wave in the direction of the receiver (red line), however even under the best circumstances a part of the signal is dispersed in other directions (blue lines).

The problem is that, as is geometrically evident, some paths are longer than others. Because of this fact, the signal is seen by the receiver multiple times with different phase shifts [5, 4]. To mathematically model this effect, we describe the received signal  $r(t)$  as a linear combination of delayed copies of the sent signal  $s(t)$ , each with a different attenuation  $c_k$  and phase shift  $\tau_k$ :

$$r(t) = \sum_k c_k s(t - \tau_k). \quad (2.5)$$

The linearity of the model is justified by the assumption that the underlying electromagnetic waves behave linearly (superposition holds) [5]. How many copies of  $s(t)$  (usually referred to as “taps” or “rays”) should be included in the formula, depends on the precision requirements of the model.

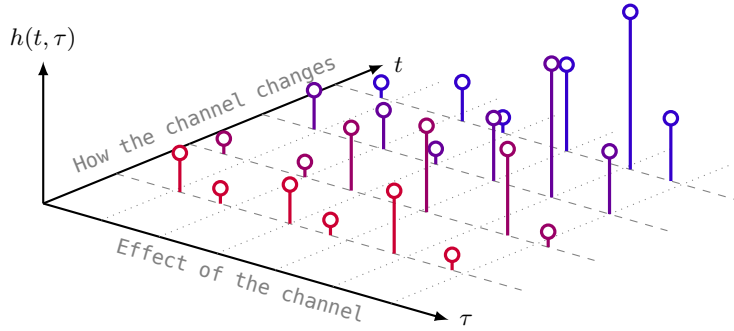


**Figure 2.5** LTV impulse response of a multipath fading channel.

A further complication arises, when one end (or both) is not stationary. In that case the lengths of the paths change over time, and as a result both the delays  $\tau_k$  as well as the attenuations  $c_k$  become functions of time:  $\tau_k(t)$  and  $c_k(t)$  respectively [5, 4]. Even worse is when the velocity at which the device is moving is high, because then Doppler shifts of the electromagnetic wave frequency become non negligible [5].

We have thus observed that the arrangement can be modelled as a linear *time-varying* system (LTV), if the sender or the receiver (or anything else in the channel) is moving, and as a linear *time invariant* (LTI) system if the geometry is stationary. Regardless of which of the two cases, linearity alone is sufficient to approximate the channel as finite impulse response (FIR) filter [4]. We can rewrite LTV version of equation (2.5) using a convolution product as following:

$$\begin{aligned} r(t) &= \sum_k c_k(t) s(t - \tau_k(t)) = \sum_k c_k(t) \int_{\mathbb{R}} s(\tau) \delta(\tau - \tau_k(t)) d\tau \\ &= \int_{\mathbb{R}} s(\tau) \sum_k c_k(t) \delta(\tau - \tau_k(t)) d\tau = s(\tau) * h(\tau, t), \end{aligned}$$

obtaining a new function

$$h(\tau, t) = \sum_k c_k(t) \delta(\tau - \tau_k(t)), \quad (2.6)$$

that describes the *channel impulse response* (CIR). This function depends on two time parameters: actual time  $t$  and convolution time  $\tau$ . To better understand  $h(\tau, t)$ , consider an example shown in figure 2.5. Each stem represents a weighted Dirac delta, so each series of stems of the same color, along the convolution time  $\tau$  axis, is a channel response at some specific time  $t$ . Along the other  $t$  axis we see how the entire channel response changes over time<sup>4</sup>. Notice that the stems are not quite aligned to the  $\tau$

<sup>4</sup>In the figure only a finite number of stems was drawn, but actually  $h(\tau, t)$  is continuous in  $t$ , i.e. the weights  $c_k(t)$  of the Dirac deltas change continuously.

## 2 Theory

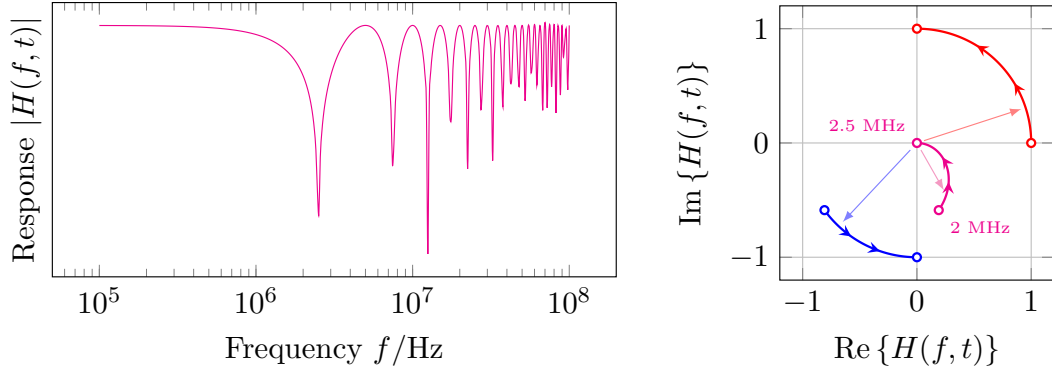


**Figure 2.6** Frequency response of a multipath fading channel.

time raster (dotted lines), that is because in (2.6) not only the weights  $c_k$  but also the delays  $\tau_k$  are time dependent.

### 2.3.2 Spectrum of a multipath fading channel

With a continuous time channel model we can now discuss the spectral properties of a fading channel since the frequency response is the Fourier transform of the impulse response, mathematically  $H(f, t) = \mathcal{F} h(\tau, t)$ . In this case however  $h(\tau, t)$  depends on two time variables, but that is actually not an issue, it just means that the frequency response is also changing with time. Hence we perform the Fourier transform with respect to the channel (convolution) time variable  $\tau$  to obtain

$$H(f, t) = \int_{\mathbb{R}} \sum_k c_k(t) \delta(\tau - \tau_k(t)) e^{-2\pi j f \tau} d\tau = \sum_k c_k(t) e^{-2\pi j f \tau_k(t)}. \quad (2.7)$$

Equation (2.7) shows that the frequency response is a periodic complex exponential, which has some important implications. Notice that if there is only one tap (term), the magnitude of  $H(f, t)$  is a constant (with respect to  $f$ ) since  $|e^{j\alpha f}| = 1$ . This means that the channels attenuates all frequencies by the same amount, therefore it is said to be a *frequency non-selective* channel. Whereas in the case when there is more than one tap, the taps interfere destructively at certain frequencies and the channel is called *frequency selective*. Plots of the frequency response of a two tap channel model are shown in Fig. 2.6. On the left is the magnitude of  $H(f, t)$ , which presents periodic “dips”, and on the right complex loci for the two taps (red and blue), as well as their sum (magenta), over the frequency range near the first dip (2 to 2.5 MHz) are shown.



### 2.3.3 Discrete-time model

Since in practice signal processing is done digitally, it is meaningful to discuss the properties of a discrete-time model. To keep the complexity of the model manageable some assumptions are necessary, thus the sent discrete signal  $s(n)$ <sup>5</sup> is assumed to have a finite single sided bandwidth  $W$ . This implies that in the time-domain signal is a series of sinc-shaped pulses each shifted from the previous by a time interval  $T = 1/(2W)$  (Nyquist rate):

$$s(t) = \sum_n s(n) \text{sinc}(t/T - n) \quad (2.8)$$

The waveform  $s(t)$  is then convolved with the CIR function  $h(\tau, t)$  (with respect to  $\tau$ ) from the continuous time model resulting in the waveform at the receiver

$$\begin{aligned} r(t) &= \int_{\mathbb{R}} \sum_n s(n) \text{sinc}(\tau/T - n) \sum_k c_k(t) \delta(\tau - \tau_k(t)) d\tau \\ &= \sum_n s(n) \sum_k c_k(t) \text{sinc}(t/T - \tau_k(t)/T - n), \end{aligned}$$

which is then sampled at the Nyquist rate of  $2W = 1/T$ , resulting in a set of samples<sup>6</sup>:

$$r(m) = \sum_n s(n) \sum_k c_k(mT) \text{sinc}(m - \tau_k(mT)/T - n).$$

Finally the substitution  $l = m - n$  eliminates the sender's sample counter  $n$  (unknown to the receiver) and reformulates  $r(m)$  as a discrete convolution product of with a discrete CIR function  $h_l(m)$ :

$$r(m) = \sum_l s(m - l) \sum_k c_k(mT) \text{sinc}(l - \tau_k(mT)/T) = \sum_l s(m - l) h_l(m). \quad (2.9)$$

This result is very similar to the continuous time model described by (2.6) in the sense that each received digital sample is a sent sample convolved with a different discrete channel response (because of time variance). To see how the discrete CIR

$$h_l(m) = \sum_k c_k(mT) \text{sinc}(l - \tau_k(mT)/T) \quad (2.10)$$

is different from (2.6) consider again the plot of  $h(\tau, t)$  in Fig. 2.5. The plot of  $h_l(m)$  would have discrete axes with  $m$  replacing  $t$  and  $l$  instead of  $\tau$ , and because of the finite bandwidth in the  $l$  axis instead of Dirac deltas there would be superposed sinc functions.

<sup>5</sup>This is an abuse of notation. The argument  $n$  is used to mean the  $n$ -th digital sample of  $s$ , whereas  $s(t)$  is used for the analog waveform.

<sup>6</sup>Again, the abusing notation  $r(m)$  means the  $m$ -th digital sample of  $r(t)$ .

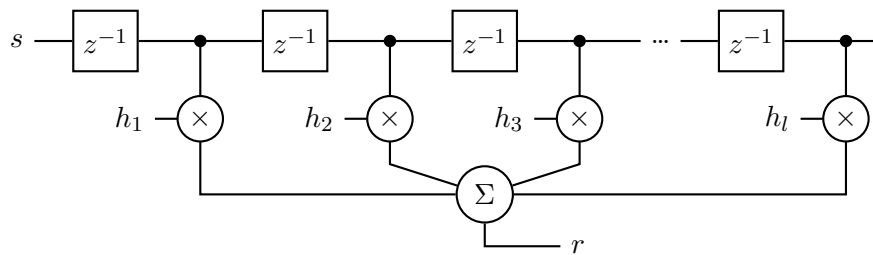


**Figure 2.7** Fading channel as a tapped delay line.

From a signal processing perspective (2.10) can be interpreted as a simple tapped delay line, schematically drawn in Fig. 2.7, which confirms that the presented mathematical model is indeed a FIR filter. Simple multipath channels can be simulated with just a few lines of code, for example the data for Fig. 2.6 is generated in just four lines of Python shown in listing 2.1. The difficulty of fading channels in practice lies in the estimation of the values for the constantly changing parameters  $c_k(t)$  and  $\tau_k(t)$ .

```
import numpy as np
```

```
def tap(c, tau, f):
    return np.exp(2j * np.pi * f * tau)
```

```
f = np.logspace(5, 8, num=320)
multipath = tap(.8, 500e-9, f) + tap(.4, 300e-9, f)
```

**Listing 2.1** Simulation of a multipath channel using a 2 tap FIR filter.

### 2.3.4 Difficulties caused by discrete time

8



9

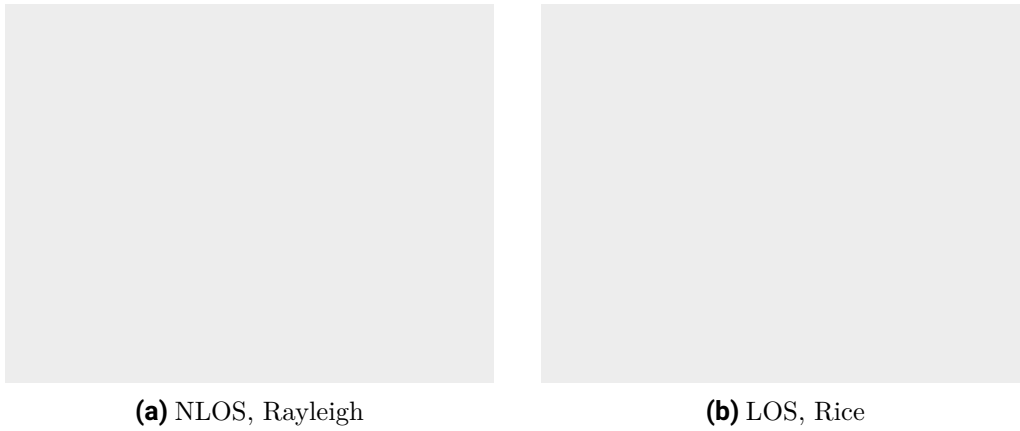


**Figure 2.8** Ring of scattering objects.



### 2.3.5 Statistical model

Because as mentioned earlier it is difficult to estimate the time-dependent parameters of  $h_l(t)$  in many cases it is easier to model the components of the CIR as stochastic processes, thus greatly reducing the number of parameters. This is especially effective for channels that are constantly changing, because by the central limit theorem the cumulative effect of many small changes tend to a normal statistical distribution.

#### NLOS case

10



$$\text{Re} \{h_l(n)\}, \text{Im} \{h_l(n)\} \sim \mathcal{N} \left( 0, \frac{1}{2} \text{E} \{|h_l(n)|^2\} \right) \quad (2.11)$$



[Redacted text]

11 LOS case

[Redacted text]

$$\text{Re}\{h_l(n)\}, \text{Im}\{h_l(n)\} \sim \mathcal{N}\left(\frac{A_l}{\sqrt{2}}, \frac{1}{2}\sigma_l^2\right) \quad (2.12)$$

[Redacted text]

# 3 Implementation

## 3.1 Overview

For the simulation task and after for the Hardware part, the open-source Software GNU Radio has been chosen. This software uses toolboxes for signal processing systems too simulate or/and implement a software-defined radio, based on Python and some C++ implementations for some rapid-application-development environments. The toolboxes can simply, with the help of the graphical user interface, used by drag-and-drop. The Boxes are used to write applications, to receive or to transmit data for a digital system. Some blocks like different filters, channel codes or demodulator elements and a lot more are already implemented. For missing application new elements can be added by coding own blocks. With the help of the GNU Radio software those toolboxes can easily get connected to each other, creating data streams.

## 3.2 Sender chain

### 3.2.1 Data source

In this simulation a random source has been chosen.

### 3.2.2 Modulation

The constellation modulator block is used for a root-raised-cosine-filtered basis modulation. The block gives an input of a byte stream as complex modulated signal in the baseband back. Further more it's possible to chose the modulation type here, in this example it is 16QAM, but QPSK, 8PSK and BPSK would also be possible.

## 3.3 Receiver chain

### 3.3.1 Envelope detector

**Polyphase Clock Sync** With the the polyphase clock sync the symbols can be synchronized by performing a time synchronization with the help of multiple filterbanks. For that the derivation of the filtered signal should be minimized which turns to a better SNR. This works with the help of two filterbanks, one of them contains the filters

### 3 Implementation

of the signal adapted to the pulse shaping with several phases. The other contains its derivative. So in the time domain it has a sinc shape, for the output Signal the sinc peak should be on a sample, with the fact that  $\text{sinc}(0) = 1$  and  $\text{sinc}(0)' = 0$  an error signal can be generated which tells how far away from the peak it is. This error Signal should be zero this is possible with the help of a loop second order which constants the number of the filterbank and the rate. This rate is generated because of the clock difference between the transmitter and receiver to synchronise the receiver the filter goes through the phases. For the output one sample per symbol is enough.

#### Equalizer

**Costas Loop** The Costas Loop is used for frequency and phase adjustment it locks the center frequency of the signal additional it converts it back to de baseband. For different modulation types different orders of the loop had to be chosen

**Constellation decoder** From the complex space the constellation points are decode to bits.

#### 3.3.2 Frame synchronization

### 3.4 Channel simulations

Here its possible to add some AWGN noise in the channel line. Different parameters can be changed like the noise voltage, time or the frequency offset.

12



To get a basic line for further simulations a 16QAM has been made. The results of this simulation are shown in Fig. 3.2 and Fig. 3.3 as the red Signal. In Tab. 3.1 some importer Parameter settings for a different modulation scheme are mentioned.

A FIR-Filter was added in the Channel to create a time delay between tow paths. In Fig. 3.2 the result includes a direct path and a delayed one. In the plot of Fig. 3.3 the transmission line doesn't include a direct path. It's impotent to mention that the delay should be smaller than the symbol rate or a multiple of it.

For the a first simulation with some fading the 16QAM simulation model has been extended with a FIR-Filter in the Chanel. The results of this simulation are shown in Fig. 3.2 and Fig. 3.3 as the blue Signal.

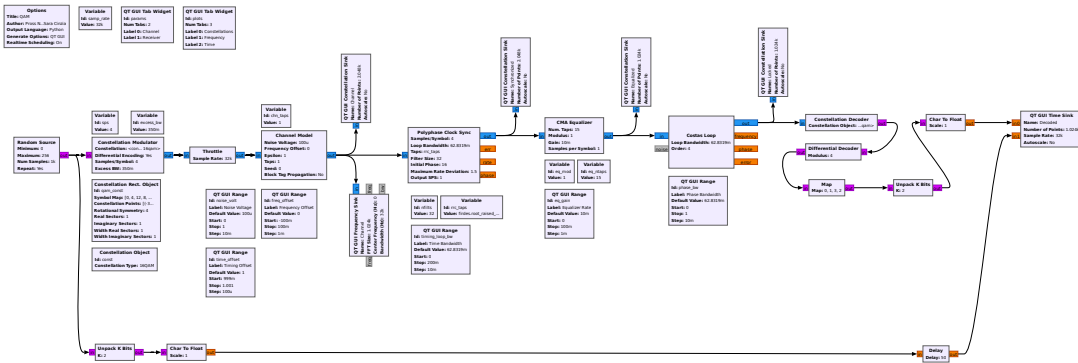


Figure 3.1 GNU Radio Blocks

Table 3.1 Modulation settings for different scheme

Modulation Scheme	Samples per Symbol	Costas Loop Order
BPSK	1	2
QPSK	2	4
8PSK	3	8
16QAM	4	4

### 3.5 Hardware

As Hardware we chosen the USRP B210 from Ettus Research, with the following specifications shown in Tab. 3.2. Because this SDR is more than enough for our requires.

For the Hardware setup up some changes are made in the file from the 16QAM simulation to fit with the SDRs. For the first test a coaxial cable was used as transmission line, after the cabel were been replaced with two antennas. The gnu radio block scheme is shown in Fig. 3.4. The results for s anntena set uo with a transmission line of 20cm are plotted in Fig. 3.5.

Instead of the channel modeling block the USRP blocks are used. The sink as transmitter and the source as resiver. The Signal is sended on a center frequency of 2.4GHz.

#### 3.5.1 Empirical BER

#### 3.5.2 Measurements

### 3 Implementation

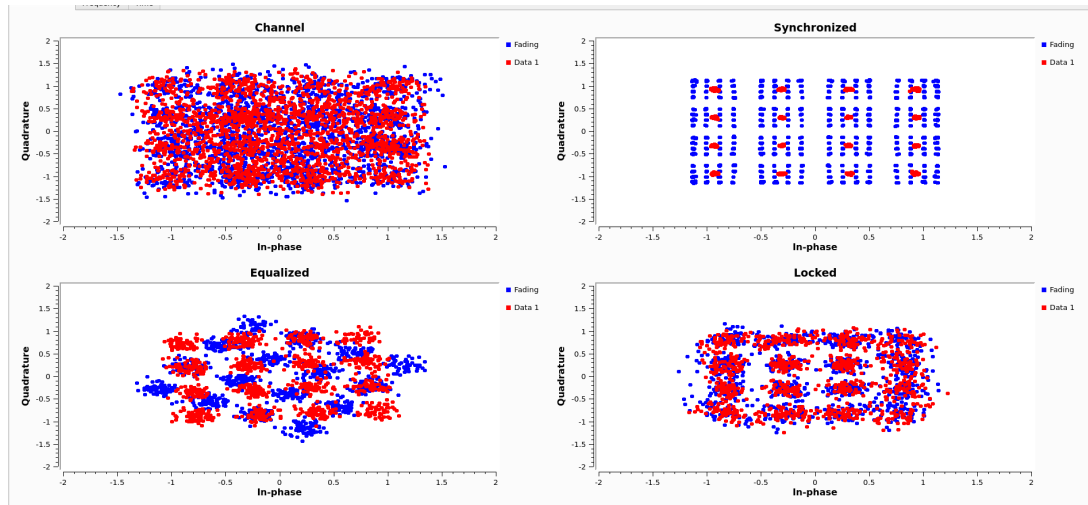


**Figure 3.2** Simulation results

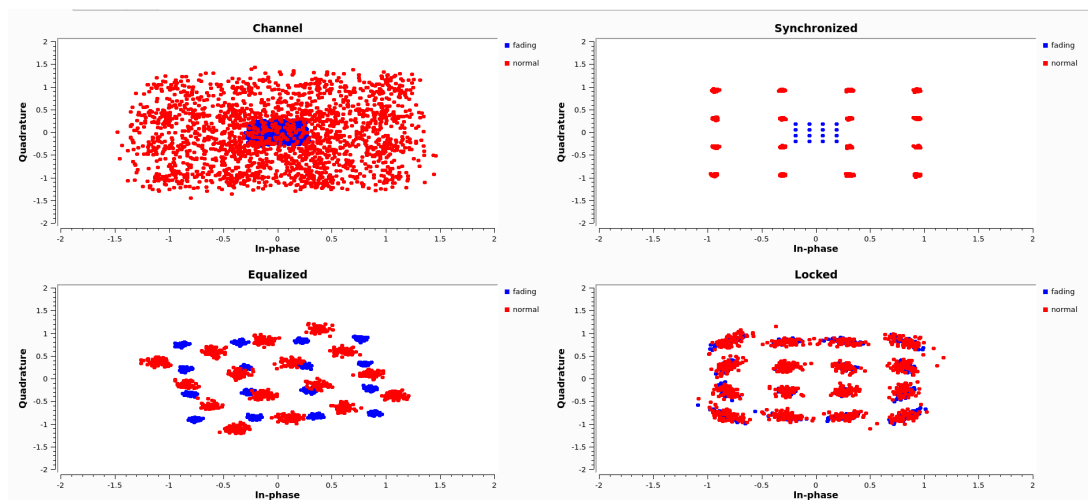


**Figure 3.3** Simulation results

**Table 3.2** USRP B210 specifications

Dimensions	$9.7 \times 15.5 \times 1.5$ cm
Ports	2 TX, 2 RX, Half or Full Duplex
RF frequencies	from 70MHz to 6GHz
Bandwidth	200kHz – 56MHz
External reference input	10 MHz



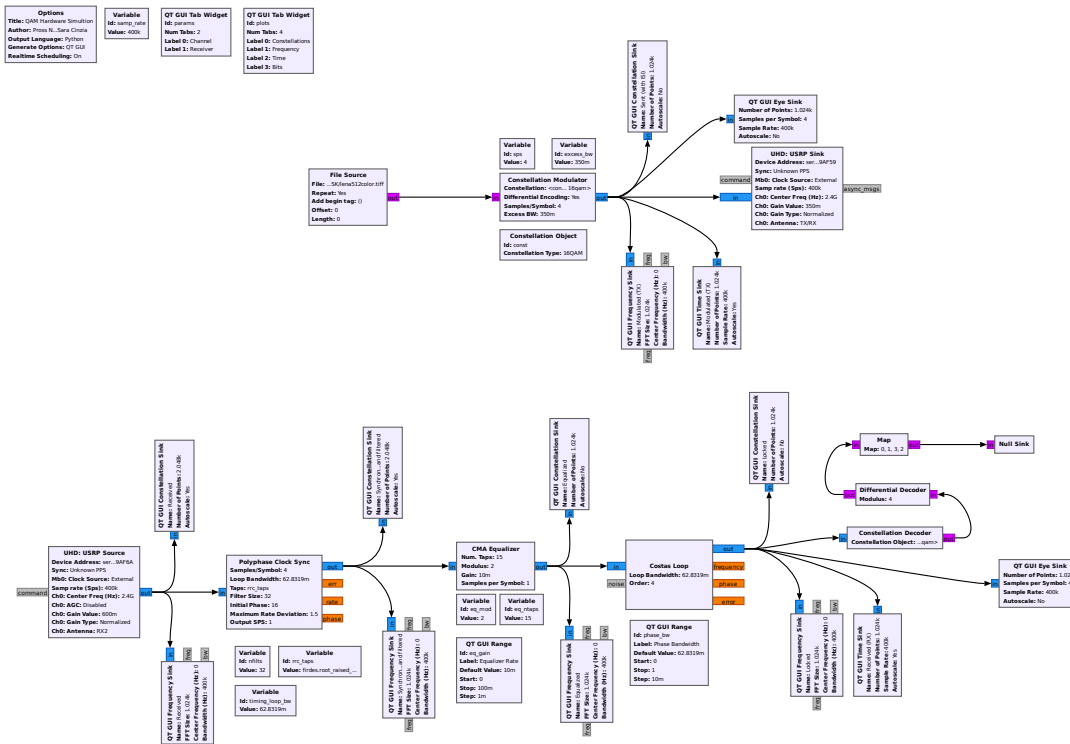


Figure 3.4 GNU Radio Blocks Hardware

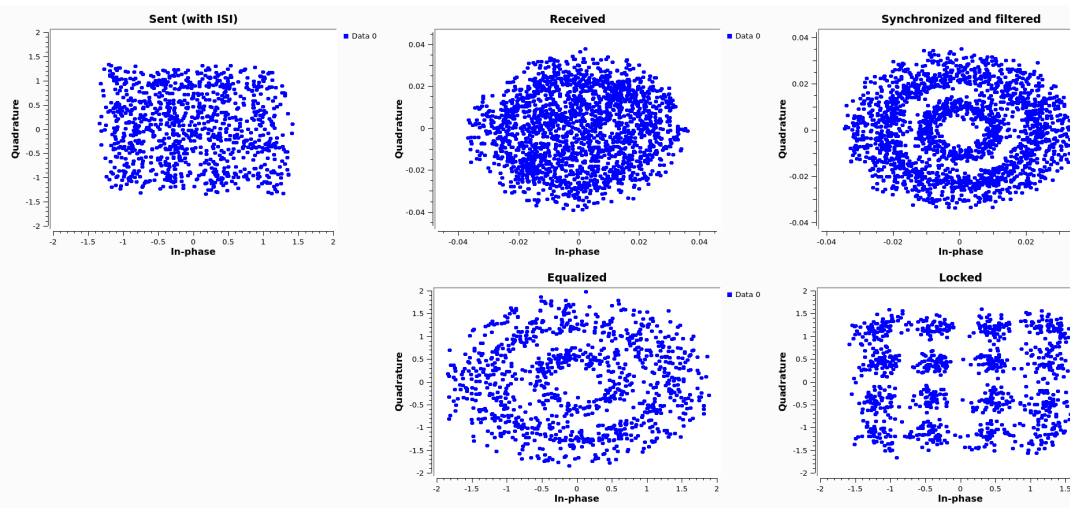


Figure 3.5 Hardware results



## **4 Conclusions**



# Notes

1. Overview of the whole document.
2. Finish overview of the chapter.
3. Discuss notation  $m(n) = m(nT)$  in discrete time and some other details.
4. Give a few details on how the carrier is generated in practice.
5. Spectral properties of QAM
6. Explain PSK (assuming the previous section was read).
7. QPSK = 4-PSK = 4-QAM
8. Not sampling at peaks of sincs.
9. Discrete frequency response. Discuss bins, etc.
10. Explain statistical model with Rayleigh distribution.
11. Explain statistical model with Rician distribution.
12. Discuss the multitap FIR model we used. How it is possible to set the delay etc. Also mathematics for the interpolation.



# Bibliography

- [1] Bogdan Antonescu, Miead Tehrani Moayyed **and** Stefano Basagni. “mmWave channel propagation modeling for V2X communication systems”. **in***2017 IEEE 28th Annual International Symposium on Personal, Indoor, and Mobile Radio Communications (PIMRC)*: 2017, **pages** 1–6. DOI: [10.1109/PIMRC.2017.8292718](https://doi.org/10.1109/PIMRC.2017.8292718).
- [2] Rob Flickenger. *Wireless Networking in the Developing World: A practical guide to planning and building low-cost telecommunications infrastructure*. Hacker Friendly LLC, Seattle, WA, US, 2007.
- [3] Flemming Bjerger Frederiksen **and** Ramjee Prasad. “An overview of OFDM and related techniques towards development of future wireless multimedia communications”. **in***Proceedings RAWCON 2002. 2002 IEEE radio and wireless conference (Cat. No. 02EX573)*: IEEE. 2002, **pages** 19–22.
- [4] Prof. Dr. Messier G. *Wireless Communications: Small Scale Fading*. 2018. URL: <https://www.youtube.com/watch?v=4ibjrRzvJ5E&list=PL7sWxFnBVJLXsvsLzMXt2Fk4ZPD7BJTBX&index=3>.
- [5] Robert Gallager. *Course material for 6.450 Principles of Digital Communications I*. Fall 2006. URL: <https://ocw.mit.edu/courses/electrical-engineering-and-computer-science/6-450-principles-of-digital-communications-i-fall-2006>.
- [6] H.P. Hsu. *Schaum's Outline of Analog and Digital Communications*. Schaum's outline series. McGraw-Hill Education, 2003. ISBN: 9780071402286.
- [7] T. Kneubühler. *Nachrichtentechnik 1 + 2*. Eastern Switzerland University of Applied Sciences, **september** 2020.
- [8] Frank R. Kschischang. “The Hilbert Transform”. **in**(**october** 2006): URL: <http://web.eecs.utk.edu/~mjr/ECE342/hilbert.pdf>.
- [9] Alex Macmillan, Mahesh K. Marina **and** Jhair Tocancipa Triana. “Slow Frequency Hopping for Mitigating Tidal Fading on Rural Long Distance Over-Water Wireless Links”. **in***2010 INFOCOM IEEE Conference on Computer Communications Workshops*: 2010, **pages** 1–5. DOI: [10.1109/INFCOMW.2010.5466612](https://doi.org/10.1109/INFCOMW.2010.5466612).
- [10] Newell C. Maddocks M.C.D. “An introduction to digital modulation and OFDM techniques”. **in***BBC Research Department*: 10 (1993).

*Bibliography*

- [11] Prof. Dr. Mathis H. **and** Prof. Dr. Lang H.D. *Wireless Communication*. Eastern Switzerland University of Applied Sciences, **september** 2021.
- [12] Lakshminarayan Subramanian **and others**. “Rethinking wireless for the developing world”. **in** *IRVINE IS BURNING*: (2006), **page** 43.